

Dendrite and fractal patterns formed on the surface of bismuth-ion-implanted LiNbO_3

This article has been downloaded from IOPscience. Please scroll down to see the full text article.

2001 J. Phys.: Condens. Matter 13 5893

(<http://iopscience.iop.org/0953-8984/13/26/304>)

View [the table of contents for this issue](#), or go to the [journal homepage](#) for more

Download details:

IP Address: 171.66.16.226

The article was downloaded on 16/05/2010 at 13:51

Please note that [terms and conditions apply](#).

Dendrite and fractal patterns formed on the surface of bismuth-ion-implanted LiNbO_3

F Chen^{1,3}, K M Wang¹, B R Shi^{1,2} and H Hu¹

¹ Department of Physics, Shandong University, Jinan 250100, China

² Department of Physics, University of Osnabrück, D-49069 Osnabrück, Germany

E-mail: drfchen@sdu.edu.cn

Received 1 December 2000, in final form 16 May 2001

Abstract

The formation of dendrite and fractal patterns on the surface of 350 keV bismuth-ion-implanted LiNbO_3 samples is presented. The dimensions of the dendrite and fractal patterns are 1.86 ± 0.04 and 1.84 ± 0.02 , respectively. For two different growth forms in our system we give some interesting experimental data. According to their morphologies, the two kinds of structure are considered to be diffusion-limit-aggregation-like patterns and dense branching morphologies, respectively. A possible origin of the dendrite and fractal patterns is also presented in a preliminary manner.

The dendrite and fractal patterns formed in non-equilibrium growth processes in physics, chemistry and biology [1] are conspicuous and many attempts have been made to investigate the mechanisms of their growth. Much work has been done to study this issue using both theoretical and experimental approaches. Up to now the basic growth modes known for fractals have been diffusion-limited aggregation (DLA) [2], the dielectric breakdown model (DBM) [3] and cluster-diffusion-limited aggregation (CDLA) [4, 5]. As a basis for understanding a wide range of pattern-formation phenomena, the DLA mode continues to play an important role in the study of fractal and dendrite formation. In addition, patterns called dense branching morphologies are frequently observed in surface growth phenomena and have been paid more attention in the field of fractal/dendrite study. Considerable effort has been devoted to experimental studies and many data have been obtained by various methods such as electrochemical deposition [6–8], acid erosion [9], fluid–fluid displacement [10] and ion implantation [11–13].

Ion implantation technology is a very important technique for studying the modification of material properties [14]. As a process far from equilibrium, ion implantation can be a suitable method for inducing random pattern growth in solid materials. So particular attention has been focused on the study of the formation and growth of dendrite and fractal structures by means of ion implantation. Dendrite and fractal patterns have been found in the surface regions of metal films [11, 12] and semiconductors [13] by ion implantation under certain experimental

³ Author to whom any correspondence should be addressed. Fax: +86 531 856 5167.

conditions. However, there is still no report on the formation of dendrite and fractal patterns on insulators by means of ion implantation. In the present work, we present an experimental study of fractal formation on the surface region of bismuth-ion-implanted LiNbO_3 samples at 350 keV for four different doses. The possible influence of dose on the properties of dendrite and fractal patterns is also discussed.

The X-cut LiNbO_3 samples with the size of $7 \times 5 \times 2.5 \text{ mm}^3$ were optically polished. They were implanted at 350 keV at room temperature with doses of 3×10^{15} , 5×10^{15} , 2×10^{16} and $3 \times 10^{16} \text{ Bi}^+$ ions cm^{-2} . The mean projected range is about 120 nm for 350 keV bismuth ions implanted into LiNbO_3 according to the TRIM 98 code. After implantation the samples were observed using a scanning electron microscope (SEM). A virgin LiNbO_3 sample was also scanned by the SEM for comparison. Furthermore, the Rutherford backscattering spectrometry (RBS)/channelling technique was used to characterize the LiNbO_3 samples. In order to determine the composition of the dendrite and fractal patterns, wavelength-dispersive spectra (WDS) obtained with an electron probe x-ray microanalyser were used to identify the patterns on the surface.

Following the implantation with doses from 3×10^{15} to $3 \times 10^{16} \text{ Bi}^+$ cm^{-2} , the surface of the LiNbO_3 samples was almost completely or partly amorphized. Figure 1 shows the RBS/channelling spectra for LiNbO_3 implantation with 350 keV Bi^+ ions with different doses. For comparison, random and channel spectra for virgin LiNbO_3 are also included. This figure reveals that a large amount of damage occurred on the surface region of the samples, including the generation of a large number of defects in the same region [14].

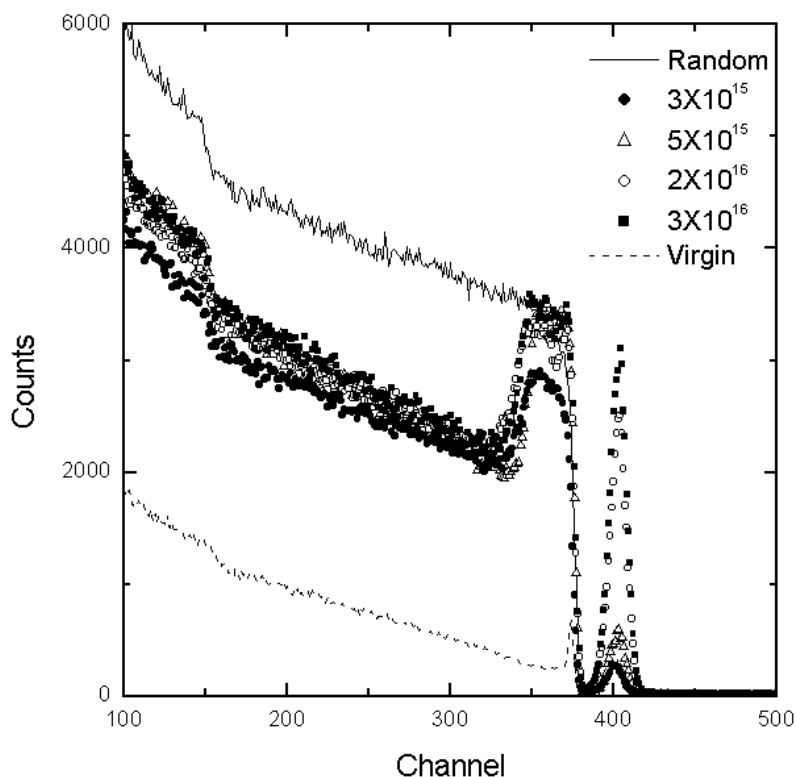


Figure 1. The RBS/channelling spectra for X-cut LiNbO_3 induced by 350 keV Bi^+ ions at doses from 3×10^{15} to 3×10^{16} ions cm^{-2} at room temperature.

A careful analysis of SEM spectra revealed that a number of dendrite and fractal structures were formed on the surface of implanted LiNbO₃ samples while no special patterns were observed on the surface of the unimplanted LiNbO₃ sample. Figure 2 shows a typical dendrite pattern observed in a bismuth-ion-implanted LiNbO₃ sample at a dose of $5 \times 10^{15} \text{ Bi}^+ \text{ cm}^{-2}$. The size of the pattern is about $1.5 \mu\text{m}$ in radius as determined from the SEM magnification. It appears as a symmetrically branched shape and it shows a nice dendrite pattern. Similar morphologies were also found on the surfaces of the other samples. On the surfaces of the samples a different kind of fractal structure was also observed. Figure 3(a) shows the typical fractal pattern with a size $7 \mu\text{m}$ in radius on the surface of the sample at a dose of $3 \times 10^{16} \text{ Bi}^+ \text{ cm}^{-2}$. At the end of each arm, other branches have generated shapes similar to the original ones, but they show a much smaller width. This case shows a typical image induced by fractal growth. Many smaller fractal structures aggregate and create a larger ball-like cluster, as shown in figure 3(b). From the electronic microscopy, the fractal patterns, displayed in figures 3(a) and 3(b), are much brighter than the dendrite structures shown in figure 2. However, our WDS analysis showed that the compositions of the two shapes were the same. These structures, in fact, were both composed of niobium particles. The difference among the dendrite and fractal patterns observed on the surfaces of the samples for the four doses is that the average sizes of the structures are different. The average size is a function of

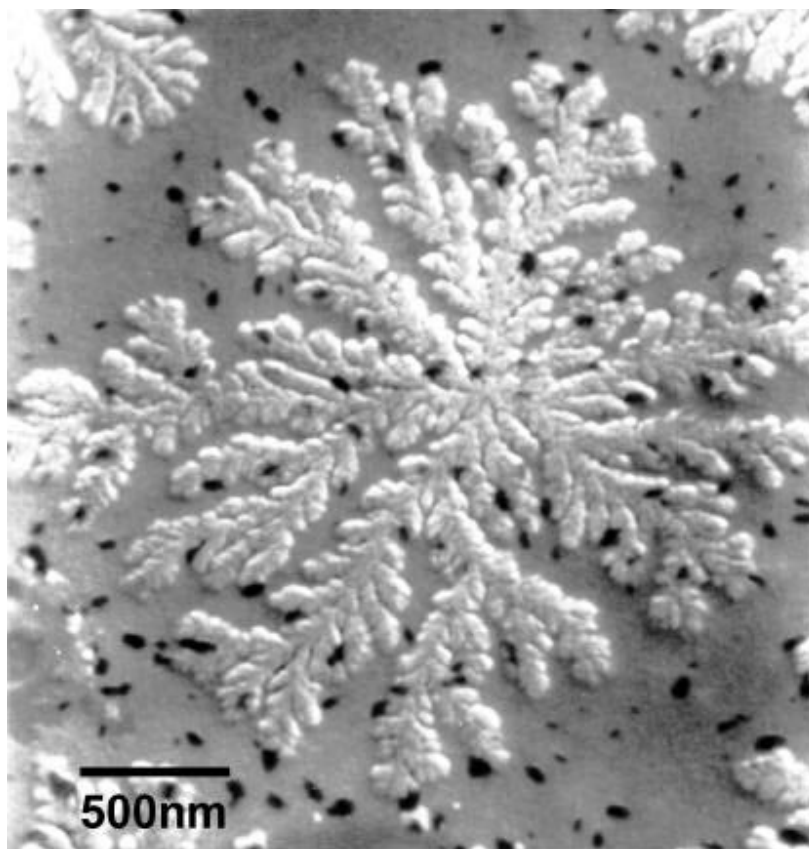


Figure 2. A typical dendrite pattern found on the surface of LiNbO₃ implanted with Bi⁺ at 350 keV to a dose of $5 \times 10^{15} \text{ ions cm}^{-2}$.

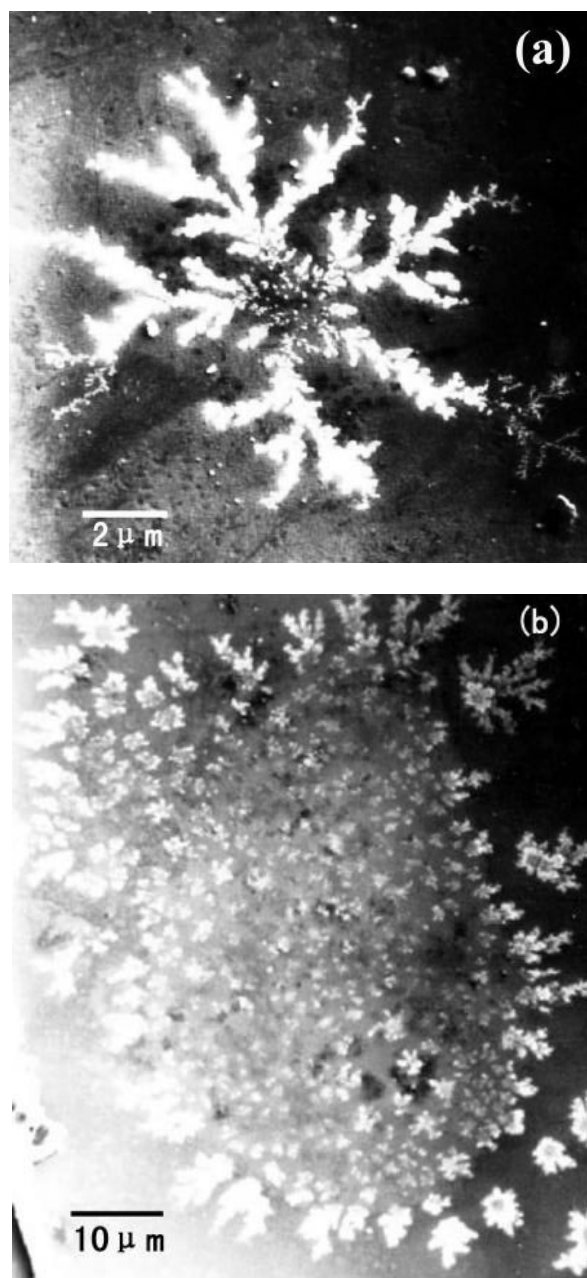


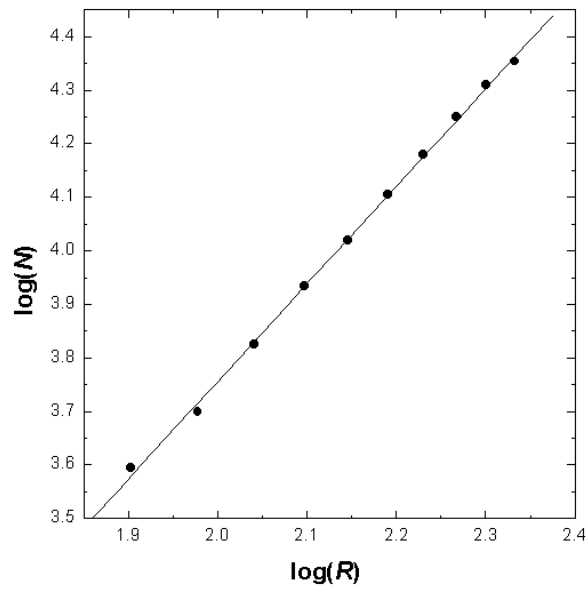
Figure 3. (a) A typical fractal pattern observed on the surface of LiNbO₃ implanted with Bi⁺ at 350 keV to a dose of 3×10^{16} ions cm⁻². (b) A large fractal ball-like cluster formed on the surface of LiNbO₃ implanted with Bi⁺ at 350 keV to a dose of 3×10^{16} ions cm⁻².

the dose for dendrite and for fractal patterns. For dendrite, the sizes of the patterns observed in LiNbO₃ implanted with 3×10^{16} Bi⁺ cm⁻² were up to ~ 7 μm in radius while those in LiNbO₃ implanted with 3×10^{15} Bi⁺ cm⁻² were only ~ 1 μm in radius. In the case of fractal structures similar to those in figure 3(a), the sizes of the patterns observed in LiNbO₃ implanted

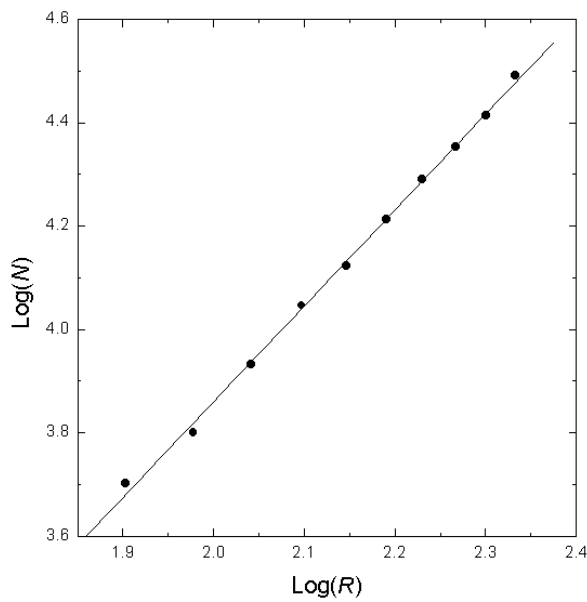
with $3 \times 10^{16} \text{ Bi}^+ \text{ cm}^{-2}$ were up to $\sim 7 \mu\text{m}$ in radius and those in LiNbO₃ implanted with $3 \times 10^{15} \text{ Bi}^+ \text{ cm}^{-2}$ were only $\sim 0.6 \mu\text{m}$ in radius. In addition, the patterns shown in figures 3(a) and 3(b) are unstable. After seven days we used SEM to investigate the state of the surfaces of the samples for a second time; the patterns had evolved towards disconnected structures.

The fractal analysis was performed therefore by digitizing the patterns in an image-processing computer with a resolution of 512×512 pixels. We used the box-counting method mentioned in reference [7] to characterize the dimensions of the fractals. They were measured by dividing the patterns into concentric discs with various radii R , and by counting the occupied pixels. The occupation numbers scaled as N ($\ln N \propto \ln D$), where D is the fractal dimension. Figure 4 shows a log–log plot of N versus R corresponding to (a) figure 3(a) and (b) figure 2. A dimension of 1.84 ± 0.02 can be extracted from figure 4(a). We have applied the same procedure to some other similar fractal patterns, and we have found that they showed almost the same value of D . We also measured the dimension of the dendrite pattern of figure 2 and a value of $D = 1.86 \pm 0.04$ was obtained from the data reported. It is important to stress that the dimension values of the observed patterns remained constant for different ion doses. This property is not only a characteristic of the patterns of figure 2 but is also shown by other structures similar to those in figure 3(a). Since the morphologies and the dimension values of the two kinds of pattern are different from each other, this suggests that two different processes occurred in the growth of the patterns. From comparison to the value for the DLA mode ($D = 1.76$), it seems to be reasonable to describe structures similar to those shown in figure 3(a) as DLA-like patterns, while for the other structures, like those reported in figure 2, the observed features strongly suggest that a dense branching morphology is a more appropriate description than DLA-like clusters.

Some previous publications reported that the fractal and dendrite patterns are frequently observed on an amorphous background. This implies that an amorphous structure could be considered to play a very important role in the formation of fractal and dendrite patterns. From this viewpoint, Liu *et al* [11, 12] proposed that the fractal dendrite patterns are due to a specific growth mode being excited in the isotropic amorphous matrix. In our work, the LiNbO₃ samples were implanted with doses ranging from 3×10^{15} to $3 \times 10^{16} \text{ Bi}^+ \text{ cm}^{-2}$ at 350 keV at room temperature. The surface regions were almost completely amorphized or partly amorphized by the strong bismuth-ion irradiation and therefore a large number of defects were induced in these regions. This revealed the basic formation situation for fractal and dendrite patterns. As we used SEM to investigate the whole surface region, we found that large areas of fractal and dendrite patterns were formed around some defects. Because there were two different morphologies observed at the same time, it seemed reasonable to assume that two kinds of process happened simultaneously which depended on different mechanisms. Furthermore, we believe that the formation and growth of the fractal and dendrite patterns induced by ion implantation are dependent on the species of the implanting ions. On the surface of LiNbO₃ implanted with Ag, Cu, Fe [16] or Au [17] ions there are only many block-like precipitates of Ag, Cu, Fe or Au to be observed rather than dendrite or fractal patterns, even when the surfaces of the samples in these cases are almost completely amorphous or partly amorphous too. Here it should be noted that bismuth ions have high polarizability, and the polarizability of the ion may play an important role in the growth of dense branching morphologies; see reference [1]. We suppose that the niobium particles have moved from their original sites following the growth of the defects. Some of the niobium particles undergo a random walk, accumulating to form fractal structures of various shapes along the direction of some defect growth, while the others aggregate into branches to fill the space uniformly, forming dense branching morphologies. With the increase of the ion doses, both dendrite and fractal patterns become larger and larger, while preserving their self-similarity. But unfortunately the direct



(a)



(b)

Figure 4. A log–log plot of N versus R for the fractal pattern in (a) figure 3(a) and (b) figure 2; R is the radius of the concentric circles in pixels and N is the number of pixels in which the surface is covered by niobium fractals in such circles.

driving force for the motion of niobium particles has not been identified, and so describing the patterns observed in nature is clearly still difficult.

As mentioned above, the fractal patterns are unstable while the dendrite patterns are relatively stable. Upon exposure to the electron beam of the SEM, although the fractal and

dendrite structures still retained their shape, the colours of the structures became darker. Further investigation shows that after seven days the fractal structures have become disconnected structures. This indicates that the formation and growth of the fractal patterns are metastable processes. We suspect that the observed shapes of the structures could be induced by the annealing caused by the electron beam. Similar fragmentation effects have been observed upon heating fractal structures to accelerate their return to equilibrium [18, 19].

Our conclusion is that there is a close relationship between the fractal/dendrite patterns and surface amorphization or partial amorphization process. Moreover, the high polarizability of the implanted Bi⁺ ions may play an important role in the growth of the dendrite patterns. The two kinds of pattern formed on the surface of 350 keV Bi⁺-implanted LiNbO₃ samples are considered to be DLA-like clusters and dense branching morphologies. We have also suggested that the fractal/dendrite formation on ion-induced insulators could be related to the species of the implanting ions, although a precise interpretation of the growth processes of these patterns is far from being achieved. The present results demonstrate the great potential of the ion implantation method for investigation of the formation of fractal and dendrite patterns.

Acknowledgments

The authors would like to thank Professor B X Liu of Tsinghua University for helpful discussion, J H Zhang, J T Liu and X D Liu for the RBS/channelling measurement, S X Shang of Shandong University Experimental Centre for SEM investigation and D R Zhang of Shandong Province Measurement Centre for WDS measurement and the calculation of the fractal dimension. This project was supported by the National Natural Science Foundation of China (grants No 19775031 and No 19875032).

References

- [1] Meakin P 1998 *Fractal, Scaling and Growth Far from Equilibrium* (Cambridge: Cambridge University Press)
- [2] Witten T A and Sander L M 1980 *Phys. Rev. Lett.* **47** 1400
Witten T A and Sander L M 1981 *Phys. Rev. Lett.* **47** 1400
Witten T A and Sander L M 1983 *Phys. Rev. B* **27** 5686
- [3] Niemeyer L, Pietronero L and Wiesmann H J 1984 *Phys. Rev. Lett.* **52** 1033
- [4] Meakin P 1983 *Phys. Rev. Lett.* **51** 1119
- [5] Kolb M, Botet R and Jullien R 1983 *Phys. Rev. Lett.* **51** 1123
- [6] Sawada Y, Dougherty A and Gollub J P 1986 *Phys. Rev. Lett.* **56** 1260
- [7] Grier D, Ben-Jacob E and Sander L M 1986 *Phys. Rev. Lett.* **56** 1264
- [8] Brune H, Romainczyk C, Roder H and Kern K 1994 *Nature* **369** 469
- [9] Ding J R and Liu B X 1989 *J. Phys.: Condens. Matter* **2** 1971
- [10] Stokes J P, Weitz D A, Gollub J P, Dougherty A, Brobbins M O, Chaikin P M and Lindsay H M 1986 *Phys. Rev. Lett.* **57** 1718
- [11] Liu B X, Huang L J, Tao K, Shang C H and Li H D 1987 *Phys. Rev. Lett.* **59** 745
- [12] Liu B X and Tao K 1993 *Nucl. Instrum. Methods B* **80/81** 332
- [13] Zhang T H and Wu Y G 1997 *Sci. China E* **27** 304
- [14] Townsend P D, Chandler P J and Zhang L 1994 *Optical Effects of Ion Implantation* (Cambridge: Cambridge University Press)
- [15] Shang C H and Liu B X 1989 *J. Phys.: Condens. Matter* **1** 10 187
- [16] Shang D Y, Yukinori S and Shinji S 1994 *Japan. J. Appl. Phys.* **33** 966
- [17] Shang D Y, Matsuno H, Saito Y and Suganomata S 1996 *J. Appl. Phys.* **80** 406
- [18] Brechignac C, Cahuzac P, Carlier F, de Frutos M, Masson A, Colliex C, Mory C and Yoon B 1997 *Z. Phys. D* **40** 516
- [19] Thouy R, Olivi-Tran N and Jullien R 1997 *Phys. Rev. B* **56** 5321